An ultra-wideband power amplifier designed through a bandwidth expansion strategy

Xuefei Xuan[1,2,3] (ID), Zhiqun Cheng[1,4] (ID), Brendan Hayes[3], Zhiwei Zhang[1] (ID), Tingwei Gong[1] (ID), Shenbing Wu[2] and Chao Le[1]

[1]The School of Electronics and Information, Hangzhou Dianzi University, Hangzhou, China; [2]The School of Electronic Engineering, Huainan Normal University, Huainan, China; [3]The School of Electronic Engineering, Dublin City University, Dublin, Ireland and [4]The School of Information Engineering, Xinjiang Institute of Technology, Xinjiang, China

Abstract

A bandwidth expansion strategy for ultra-wideband power amplifiers (PAs) is presented in this letter by adopting a parallel impedance matching architecture. This design strategy can effectively reduce the impedance conversion ratio between the load and the target impedance of the PA, thereby providing a feasible solution for broadband impedance matching. Subsequently, a commercially available 10 W gallium nitride device and a two-stage Wilkinson power divider network are combined to achieve the verification of the proposed theory. The results of the measurement show that within the target frequency band of 0.9–3.9 GHz, 58.5–71.2% of the drain efficiency and 9.1–12 dB of gain can be achieved with a saturated output power of 39.1–42 dBm.

Introduction

The next generation of wireless communication systems is required to operate on different frequency bands for different applications. Taking mobile communication as an example, the arrival of the fifth generation (5G) communication era has led to an increasing number of high-frequency bands being included in the communication frequency band. Therefore, as a core component of the communication system, power amplifiers (PAs) are required to operate efficiently over a wide frequency band [1–5].

The continuous mode [6–8], developed based on harmonic-tuning technology, is considered one of the most promising bandwidth expansion technologies at present. However, considering that relying solely on expanding the target impedance space is difficult to satisfy the practical application requirements in the context of ultra-wideband operation required by 5G communication, improving the impedance matching network has become an effective way to expand the operating bandwidth of PAs, such as simplifying real-frequency technology [9, 10] and distributed matching networks [11, 12], which have been proven to have outstanding performance in broadband impedance matching. Among them, simplified real frequency technology is to find a suitable impedance matching path through algorithm optimization to complete the matching between load and target impedance of PA in a wide frequency band, as shown in papers [9, 10]. Distributed filtering matching networks are usually based on low-pass or band-pass filtering networks, which are synthesized or improved into impedance matching networks with broadband responses to achieve bandwidth expansion of PAs, such as papers [11, 12]. However, it can be found that neither optimization algorithms represented by simplified real frequency nor distributed filtering networks can be directly used for matching network design, and it is necessary to first convert the lumped parameters into distributed parameters. The conversion of lumped components to transmission lines will introduce errors, and further optimization is needed to reduce the errors caused by the conversion. As a result, the design complexity of PAs will be increased.

In this letter, a bandwidth expansion design strategy is proposed to achieve the design of an ultra-wideband PA operating at 0.9–3.9 GHz by using a parallel impedance matching architecture. The measured results indicate that within the target frequency band, 58.5–71.2% of the drain efficiency (DE), 39.1–42 dBm of output power, and 9.1–12 dBm of gain are achieved.

Design theory

The difficulty of bandwidth expansion in ultra-wideband PAs depends on the conversion ratio between the load and the target impedance. Generally speaking, the larger the difference between the load and target impedance, the more difficult it will be to maintain good impedance matching within wideband. Therefore, the key to implementing ultra-wideband PAs lies in designing impedance matching networks to reduce the conversion ratio from load to target impedance. Based on this design concept, a novel parallel impedance
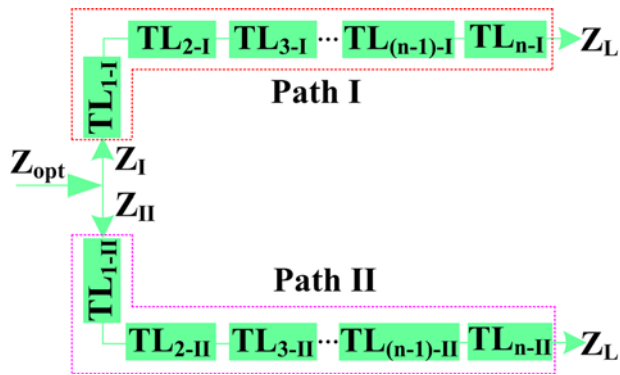
Figure 1. Schematic diagram of proposed parallel impedance matching architecture.

Figure 2. Optimal impedances distribution for load in 1.0–4.0 GHz.

matching architecture is proposed to reduce the load to target impedance conversion ratio, as shown in Fig. 1. The presented parallel impedance matching architecture consists of two matching paths, each of which is composed of an undetermined number of series transmission lines, used to achieve the matching of load impedance Z_L to impedance Z_I and Z_{II} by employing the principle of transmission line impedance transformation [13].

As a result, the input impedance Z_{opt} can be calculated as follows:

$$Z_{opt} = (Z_I \bullet Z_{II}) / (Z_I + Z_{II}) \tag{1}$$

Assuming Z_I and Z_{II} are considered pure resistors, equation (1) can be transformed as follows:

$$Z_{opt} = (Z_I \bullet Z_{II}) / (Z_I + Z_{II}) \leq (Z_I + Z_{II}) / 4 \tag{2}$$

Therefore, it can be observed that the impedance achieved through two parallel impedance matching architectures is always less than or equal to a quarter of the sum of the impedances matched in paths I and II, respectively. Only under the condition of $Z_I = Z_{II}$, can equality be obtained, which means that even if the input impedance Z_{opt} is taken as the maximum, it is only half of Z_I or Z_{II}. As a result, under this condition, the impedance conversion required for the proposed parallel impedance matching architecture is directly reduced by 50% compared to conventional impedance matching networks, which is extremely advantageous for achieving ultra-wideband impedance matching.

Realization of ultra-wideband PA

In this section, based on the proposed parallel impedance matching architecture, an ultra-wideband PA operating at 0.9–3.9 GHz is designed using a commercially available 10 W gallium nitride (GaN) device provided by Cree, and the gate and drain bias voltages are set at −2.7 V and 28 V, respectively.

Acquisition of optimal impedance

The design of ultra-wideband PAs starts with achieving the target impedance within the design frequency band. Based on the current application requirements of wireless communication systems, PAs are required to work efficiently on a wide frequency band, so obtaining the target impedance is particularly important. In terms of efficiency improvement, considering the presence of harmonics, especially second harmonics, is crucial. In PA design,
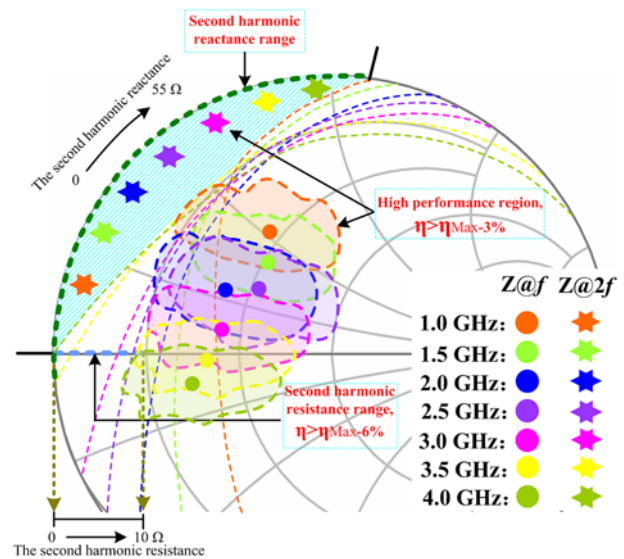
using load-pull technology to achieve the target impedance at the design frequency point is a common technical means, while the analysis of the second harmonic impedance is ignored, which leads to the inability to further ensure the efficiency of PA while completing bandwidth expansion. In view of this situation, to incorporate the second harmonic into the analysis of the target impedance, the multi-harmonic bilateral pull technique [14] is employed to achieve the fundamental and second harmonic impedances, providing design goals for the implementation of ultra-wideband PAs.

Then, based on the commercially available transistor model CGH40010F, the multi-harmonic bilateral pull technology is implemented at the device output for 1.0–4.0 GHz. As a result, the optimal fundamental and second harmonic impedance regions from the target frequency band are obtained, as shown in Fig. 2, where the internal regions of the fundamental and second harmonic impedance curves represent the tolerable regions for achieving high efficiency. In addition, more importantly, it can be observed from Fig. 2 that the second harmonic impedance region of the entire target frequency band is not limited to pure reactance but is extended to resistance-reactance under acceptable operating efficiency performance. Specifically, the imaginary part reactance varies between 0 and $55\,\Omega$, while the real part resistance is extended between 0 and $10\,\Omega$, which is consistent with the conclusion of the extended continuous mode [7] or inverse mode [15]. Based on this, it can be inferred that by selecting the target impedance region reasonably, the overlap between the second harmonic impedance and the fundamental impedance is allowed, indicating that maintaining good efficiency performance while completing bandwidth expansion can be achieved. So far, the target impedance of the design frequency band has been determined, and the next step is to complete the design of the ultra-wideband PA based on the parallel impedance matching architecture proposed in section "Design theory."

Design of ultra-wideband PA

Based on the target impedance obtained by combining the proposed parallel impedance matching architecture, the design of the ultra-wideband PA can be implemented. However, there are
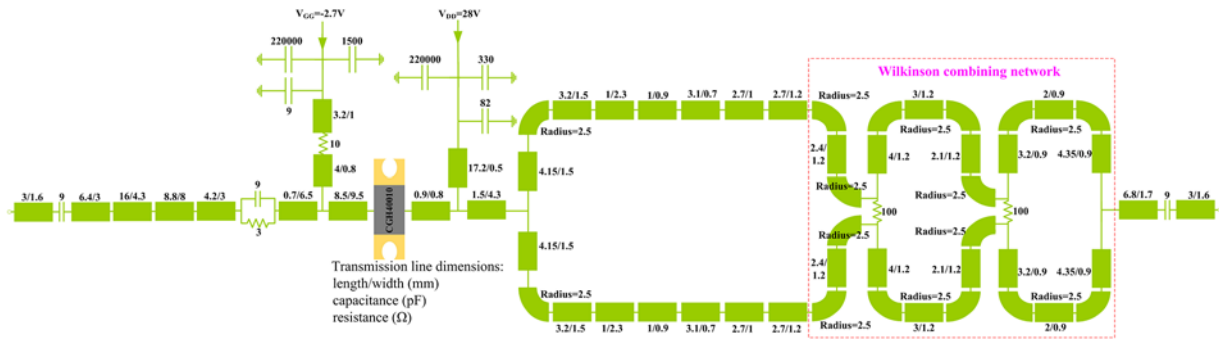
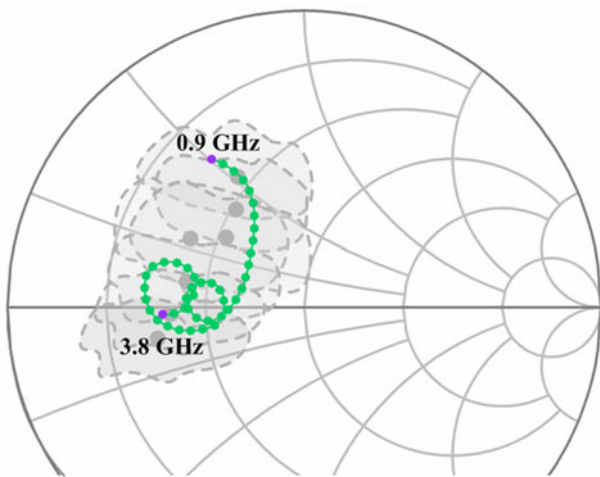**Figure 3.** Schematic of the designed PA. Dimensions are in mm.

Figure 4. Impedance trajectory completed by output matching network.
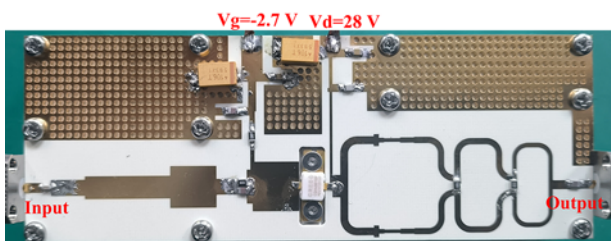

Figure 5. Fabricated PA circuit.

two issues that need further discussion before this. Firstly, according to the proposed parallel impedance matching architecture, how to maintain the terminal impedance of two matching paths as the load impedance within the target frequency band. Considering the need to maintain good isolation between parallel impedance matching architectures and the ability of two signals to overlap in the same direction at the synthesis point, the Wilkinson combining network is chosen for use [13]. As long as a good input reflection coefficient is maintained at the input terminal of the Wilkinson power divider network, the terminal impedance of the matching path can be well maintained as Z_L. Here, the microwave system impedance is used as a reference, which is 50 Ω. Specifically, in order to further expand the operating bandwidth of the Wilkinson power divider network, a two-stage cascaded architecture is chosen [13].
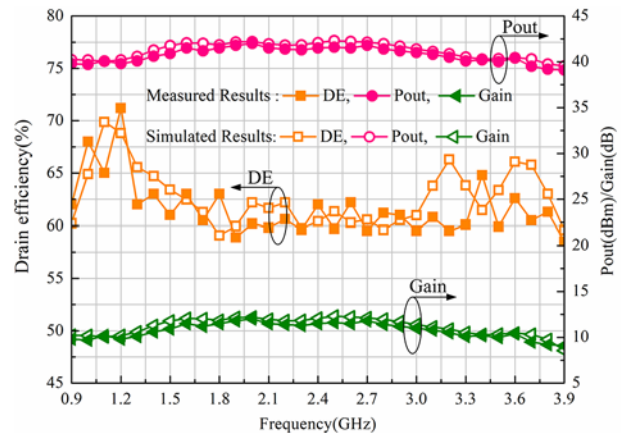

Figure 6. Measured and simulated DE, output power, and gain (at saturation) vs. frequency.

Secondly, how to consider the topology selection of two matching paths. In the theoretical analysis in section "Design theory," we pointed out that even if the input impedance of the two paths is set to be the same, as in the most general case, compared with traditional impedance matching networks, the proposed parallel impedance matching structure can still reduce the impedance conversion ratio by 50%. Therefore, the scheme of using the same impedance matching network for two matching paths is considered. In this way, the design complexity of the entire circuit will also be greatly reduced. As a result, the topology structure of the designed ultra-wideband PA is shown in Fig. 3.

Figure 4 shows the impedance trajectory completed by the output matching network. It can be observed from the figure that the completed impedance gradually moves toward the lower part of the Smith Circle with increasing frequency starting from 0.9 GHz, which is consistent with the trend of the target impedance varying with frequency. And it is basically located in the target impedance region, indicating the rationality of the impedance matching network design.

Fabrication and measurement of PA

The photograph of the fabricated ultra-wideband PA is demonstrated in Fig. 5 on a Rogers 4350B substrate.

To further verify the frequency response of the designed ultra-wideband PA, measurement of the PA is performed using continuous waveform signals from 0.9 to 3.9 GHz. Based on this, the

Table 1. Comparisons with state-of-the-art broadband PAs

Ref	Technology	BW (GHz)	RBW (%)	DE (%)	Power (dBm)	Gain (dB)	Static operating points	Type of transistor	Year
[16]	SCMs	1.6–2.8	54.5	67.5–81.9	39.08–42.5	NA	$Vg = -3$ V, $Vd = 28$ V	GaN	2014
[17]	SCMs	0.8–3.2	120	57–74	39.7–42.9	10.7–14.1	$Vg = -3$ V, $Vd = 28$ V	GaN	2018
[18]	Chebyshev low-pass network	1.9–3.1	48	48–56.6	39.3–40.5	9.3–10.7	$Vg = -3$ V, $Vd = 28$ V	GaN	2020
[19]	Particle swarm optimization	2.2–4.6	62.8	51–70	40–42.8	12.8–14.9	$Ids = 150$ mA, $Vd = 28$ V	GaN	2021
[20]	Fictitious matching	0.5–3	143	53.4–70	39.6–41.4	10.6–12.4	$Vg = -2.82$ V, $Vd = 28$ V	GaN	2022
[21]	Harmonic-controlled matching network	2.9–3.3	12.9	68.2–74.3	36–38.6	NA	$Ids = 60$ mA, $Vd = 28$ V	GaN	2023
This work	Parallel impedance matching architecture	0.9–3.9	125	58.5–71.2	39.1–42	9.1–12	$Vg = -2.7$ V, $Vd = 28$ V	GaN	2024

BW = bandwidth; RBW = relative bandwidth; SCMs = series of continuous modes.
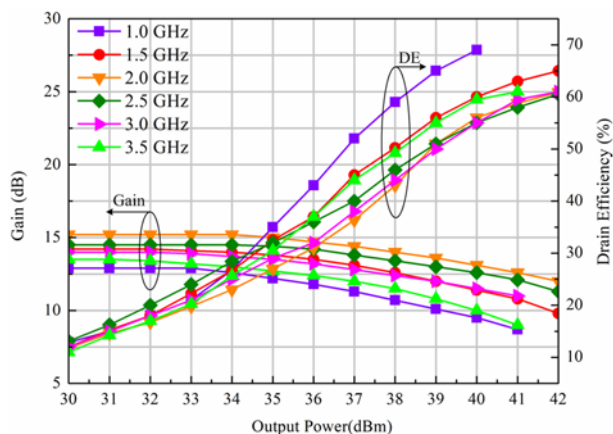
Figure 7. Measured DE and gain vs. output power for some in-band frequencies.

DE, output power, and gain achieved through measurement and simulation are plotted in Fig. 6. It can be seen that within the target frequency band of 0.9–3.9 GHz, the DE of 58.5–71.2% and the gain of 9.1–12 dB can be achieved under a saturation output power of 39.1–42 dBm. Table 1 shows that the proposed PA has a larger bandwidth compared to previously published work, fully utilizing the 10 W capability of the device.

To measure the dynamic characteristics of the implemented PA, the tested gain and DE vs. output power at six frequency points within the design frequency band are presented in Fig. 7. From the graph, it can be observed that the gain decreases with the increase in output power, while the DE shows an increase, meaning that a compromise between gain and efficiency needs to be considered in the design of PAs.

Furthermore, when the output power reaches saturation, increasing the output power further slows down the increase in DE significantly while the decrease in gain becomes more pronounced. Therefore, when saturated output is used as available power within

the target frequency band, both gain and DE are at an acceptable level.

Conclusion

An ultra-wideband PA has been designed and characterized by using a bandwidth expansion strategy that utilizes a parallel impedance matching architecture. This strategy can effectively reduce the impedance conversion ratio between the load and the target impedance, thereby achieving the goal of bandwidth expansion. The designed PA was fabricated and measured, and the test results showed that with an output power of 39.1–42 dBm, the DE of 58.5–71.2% and the gain of 9.1–12 dB can be achieved within the target frequency band of 0.9–3.9 GHz, demonstrating the feasibility of the design theory.

Author contributions. Xuefei Xuan wrote the main manuscript text and derived the theory with Zhiqun Cheng, Zhiwei Zhang and Tingwei Gong performed the simulations. Brendan Hayes is responsible for the grammar

correction of the manuscript. Shenbing Wu prepared Figs. 5–7. Chao Le prepared Figs. 1–4 and Table 1. All authors contributed equally to analyzing data and reaching conclusions, and in writing the paper.

References

1. **Zhang Z, Fusco V, Cheng Z, Buchanan N and Gu C** (2022) A quad-band power amplifier based on impedance frequency modulation. *IEEE Transactions on Circuits and Systems II: Express Briefs* **69**(3), 724–728.
2. **Latha YMA and Rawat K** (2022) Design of ultra-wideband power amplifier based on extended resistive continuous class B/J mode. *IEEE Transactions on Circuits and Systems II: Express Briefs* **69**(2), 419–423.
3. **Yang C, Jin K, Mao D and Zhu X** (2022) Precise configuration of transmission line class-E power amplifier operating at GHz frequency. *IEEE Journal of Emerging and Selected Topics in Power Electronics* **10**(5), 6396–6404.
4. **Liu W, Liu Q, Du G, Li G and Cheng D** (2023) Dual-band high-efficiency power amplifier based on a series of inverse continuous modes with second-harmonic control. *IEEE Microwave and Wireless Technology Letters* **33**(8), 1199–1202.
5. **Liu C, Li X and Ghannouchi FM** (2023) A highly-efficient Doherty power amplifier with generalized parallel-circuit class-EF mode. *IEEE Transactions on Circuits and Systems II: Express Briefs* **70**(8), 2819–2823.
6. **Sharma T, Darraji R, Ghannouchi F and Dawar N** (2016) Generalized continuous class-F harmonic tuned power amplifiers. *IEEE Microwave and Wireless Components Letters* **26**(3), 213–215.
7. **Huang H, Zhang B, Yu C, Gao J, Wu Y and Liu Y** (2017) Design of multioctave bandwidth power amplifier based on resistive second-harmonic impedance continuous class-F. *IEEE Microwave and Wireless Components Letters* **27**(9), 830–832.
8. **Zheng SY, Liu ZW, Zhang XY, Zhou XY and Chan WS** (2018) Design of ultrawideband high-efficiency extended continuous class-F power amplifier. *IEEE Transactions on Industrial Electronics* **65**(6), 4661–4669.
9. **Jung WL and Chiu J-H** (1993) Stable broadband microwave amplifier design using the simplified real frequency technique. *IEEE Transactions on Microwave Theory and Techniques* **41**(2), 336–340.
10. **Meng F, Zhu X-W, Xia J and Yu C** (2018) A new approach to design a broadband Doherty power amplifier via dual-transformation real frequency technique. *IEEE Access* **6**, 48588–48599.
11. **Xia J, Zhu X and Zhang L** (2014) A linearized 2–3.5 GHz highly efficient harmonic-tuned power amplifier exploiting stepped-impedance filtering matching network. *IEEE Microwave and Wireless Components Letters* **24**(9), 602–604.
12. **Chen K and Peroulis D** (2012) Design of broadband highly efficient harmonic-tuned power amplifier using in-band continuous class-F^{-1}/F mode transferring. *IEEE Transactions on Microwave Theory & Techniques* **60**(12), 4107–4116.
13. **Pozar DM** (1998) *Microwave Engineering*, 2nd edn. New York, NY: Wiley.
14. **Chen H and Zhang YX** (2008) Design of microwave power amplifier based on multi-harmonic bilateral-pull technology. *Journal of Microwaves* **24**(3), 57–60.
15. **Carrubba V, Akmal M, Quay R, Lees J, Benedikt J, Cripps SC and Tasker PJ** (2012) The continuous inverse class-F mode with resistive second-harmonic impedance. *IEEE Transactions on Microwave Theory & Techniques* **60**(6), 1928–1936.
16. **Chen J, He S, You F, Tong R and Peng R** (2014) Design of broadband high-efficiency power amplifiers based on a series of continuous modes. *IEEE Microwave and Wireless Components Letters* **24**(9), 631–633.
17. **Wang J, He S, You F, Shi W, Peng J and Li C** (2018) Codesign of high efficiency power amplifier and ring-resonator filter based on a series of continuous modes and even-odd-mode analysis. *IEEE Transactions on Microwave Theory & Techniques* **66**(6), 2867–2878.
18. **Haider MF, You F, Shi W, Ahmad S and Qi T** (2020) Broadband power amplifier using hairpin bandpass filter matching network. *Electronics Letters* **56**(4), 182–184.
19. **Poluri N and De Souza MM** (2021) Designing a broadband amplifier without load–pull. *IEEE Microwave and Wireless Components Letters* **31**(6), 593–596.
20. **Kilinc S, Yarman BS and Ozoguz S** (2022) Broadband power amplifier design via fictitious matching. *IEEE Transactions on Circuits and Systems II: Express Briefs* **69**(12), 4844–4848.
21. **Kim J, Hong SK and Oh J** (2023) Highly efficient power amplifier based on harmonic-controlled matching network. *IEEE Microwave and Wireless Technology Letters* **33**(1), 43–46.

Xuefei Xuan received the M.E. degree in electromagnetic field and microwave techniques from Hangzhou Dianzi University, Hangzhou, Zhejiang, China, in 2018. He is currently pursuing the Ph.D. degree with the Hangzhou Dianzi University, Hangzhou and is with the Dublin City University, as a visiting student. His research interests include the design of RF/mm-wave power amplifiers, efficiency enhancement techniques, broadband techniques, and mm-wave integration circuits and systems.

Zhiqun Cheng received the B.S. and M.S. degrees from the Hefei University of Technology, Hefei, China, in 1986 and 1995, respectively, and the Ph.D. degree in microelectronics and solid state electronics from the Shanghai Institute of Metallurgy, Chinese Academy of Sciences, Shanghai, China, in 2000. From 1986 to 1997, he was a Teaching Assistant and a Lecturer with the Hefei University of Technology, China. From 2000 to 2005, he was an Associate Professor with the Shanghai Institute of Metallurgy, China. He is currently a Professor and the Dean of the School of Electronic and Information, Hangzhou Dianzi University. He has authored or co-authored over 150 technical journal and conference papers. His research interests include microwave theory and technology, MMIC, power amplifier, and RF front end. He is currently a member of a Council of Zhejiang Electronic Society. He was also a Chair of the Organizational Committee for over 10 International Conferences.

Brendan Hayes received the B.S. degree from the Dublin City University, Dublin, Ireland, in 2013, and the Ph.D. from the Dublin City University, Dublin, Ireland, in 2016. From 2016 to 2018, he was a Postdoctoral Researcher with the University College Dublin, Dublin, Ireland. He is currently an Assistant Professor with Dublin City University. His current research interests include power electronics, nonlinear dynamics.

Zhiwei Zhang received the B.S. degree in electronic science and technology from Hangzhou Dianzi University, Hangzhou, China, in 2017, and the Ph.D. degree in electronic science and technology from the Hangzhou Dianzi University (HDU), Hangzhou, China, in 2022. He is currently an Associate Professor with HDU. His current research interests include highly linear and efficient microwave PA design.

Tingwei Gong He is currently pursuing the Ph.D. degree with Key Lab. of RF Circuit and System, Education Ministry. He is currently with the Centre for Wireless Innovation. His research interests include microwave theory and technology, MMIC, power amplifier, and RF front end.

Shenbing Wu received the M.E. degree in electromagnetic field and microwave techniques from Anhui University, Hefei, Anhui, China, in 2021. He is currently working in Huainan Normal University. His research interests include designing FSS and microwave devices.

Chao Le He is currently the project leader of Fuyang Electronic Information Research Institute Co., Ltd of Hangzhou University of Electronic Science and Technology.